Design a Cage-typed Light Field Camera System for Flame Measurement

Yudong Liu[1], Md. Moinul Hossain[2], Jun Sun[1], Chuanlong Xu*[1], Biao Zhang[1], Shimin Wang[1]
[1]School of Energy and Environment, Southeast University, Sipailou 2#, Nanjing, China.
[2]Department of Electronic and Electrical Engineering, University of Strathclyde, Royal College Building, Glasgow, G1 1XW
E-mail: yudong.liu@seu.edu.cn; m.hossain@strath.ac.uk; j_ustdoit@126.com; chuanlongxu@seu.edu.cn*;
zhangbiao@seu.edu.cn; smwang@seu.edu.cn

***Abstract*—A cage-typed light field camera system for flame temperature measurement is designed and fabricated to obtain flexibility to change its components and parameters. In this case, it is flexible to change the components of the light field camera to compare the performance of different optical parameters on the measurement accuracy of the flame. The structure and components of the cage-typed light field camera system are presented and discussed. At different parameters, their results are compared to evaluate the performance of the light field camera. The results indicate that the cage-typed system has good imaging performance for different parameters. To validate the proposed system, the self-assembled camera is utilised to retrieve the flame temperature from light field flame images through the use of deconvolution method.**

Keywords—light field; cage-typed; parameter adjusting; flame temperature measurement

I. INTRODUCTION

In three-dimensional (3-D) space, the light field describes the light transmission, which is determined by the position, the direction and the intensity of each ray of light [1]. The light field camera was designed to collect the light field of the scene. The first prototype of standard light field camera was proposed by Ng et al. [2]. In the prototype, the image sensor was assembled directly on the focal plane of the microlens array (MLA) to acquire the light field through a compact and portable device. Separation from the MLA to the image sensor of Ng's prototype is further optimised to improve the resolution of rendered images [3]. Since then, commercial light field cameras of Lytro (Ng's prototype) and Raytrix (focused light field camera) have become accessible in different applications [4, 5]. The parameters such as focal length and diameter of the microlens are usually optimizable for the different applications and but not adjustable. For instance, in the commercial light field camera of Raytrix 29, the MLA is stuck directly on the frame of CCD (a charge-coupled device) sensor, and hence the distance between MLA and the CCD sensor is fixed. Therefore, the performance of the commercial light field camera is limited in some studies such as flame temperature measurement [6]. In addition, parameters such as the diameter of the microlens are only accessible by the manufacturer not to the customers. Hence, due to the unknown parameters, the commercial light field cameras cannot be utilised in some applications where the camera calibrations are needed [7].

Therefore, it is important to design and assemble the corresponding light field camera for specific applications. The light field cameras with different structures and parameters were specially designed and assembled in various studies [7, 8]. For example, a self-assembled focused light camera is designed to obtain pro-known parameters for the validation of calibration methods [7]. Kyle et al.[8] utilised a custom mount approach to position the microlens array accurately over the sensor in the plenoptic camera for particle image velocimetry. Zhou et al. [9] stuck the MLA on the frame of CCD sensor directly for the optical analysis of their assembled light field camera. The parameters are pro-known and can be optimised numerically before manufacturing in these specially-designed light field cameras. However, the positions and tilt angles of each component are unchangeable after assembly, which means that all the lens and camera parameters are fixed. Studies reported that the flame temperature measurement using the light field camera is required to change its parameters for the accurate measurements in terms of flame radiation sampling [6]. In recent years, the light field camera has been applied to reconstruct the 3-D flame temperature using the commercial light field camera [6, 10]. However, the parameters of the light field cameras are unknown and unchangeable. Although the preliminary results of the flame temperature are obtained, it is unknown whether the performance can be improved by changing the parameters of the light field camera.

In this study, a novel cage-typed light field camera has been designed and fabricated, where the components or parameters of the light field camera are easily changeable. The structure of the cage-typed light field camera and parameters is presented and described. The images with different parameters are compared for the flame measurement. Experimental results of flame temperature are also presented using the proposed cage-typed light field camera system.

II. DESIGN & FABRICATION

A. Design structure of the Cage-type light field camera

The cage-typed light field camera consists of the main lens, MLA, relay lens and CCD sensor along with a series of adaptors for connection and attachment. All components are mounted on the cage plates and connected by four stainless steel cages rods, as shown in Fig. 1. By this way, the position of each optical components can easily be adjusted. The relay lens is used to extend the imaging distance between the MLA and the CCD sensor to decrease the difficulty of assembling and adjusting. Two Nikon 50mm f/1.8D lenses are used in the cage system and connected head-to-head, their apertures are both fixed on f/1.8 for the maximum luminous flux, and they both focused on the infinity for an accurate relay imaging. Such a symmetrical

optical structure can eliminate the aberration at a decent level. The aperture of the main lens is fixed on f/4, which equals to the aperture of the microlens. The MLA is mounted in a high-precision zoom house. The zoom house provides the ability to control the exact assembling position of the MLA. The accuracy is found 2 μm.

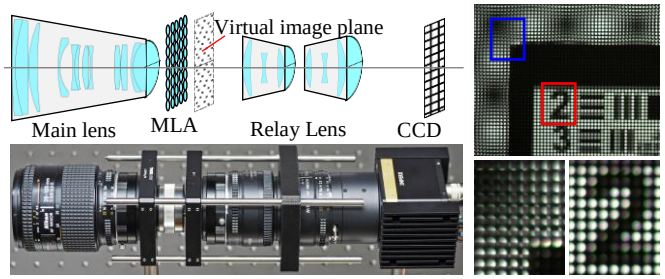

Fig. 1. The structure of the cage-typed light field camera and example of a raw image captured by the cage-type light field camera.

In the process of capturing the scene, the light is collected by the main lens, light converge and re-separate by the MLA and form an image on a plane (named as a virtual image plane in this study). The image on the virtual image plane is then relayed by the relay lens to the CCD sensor and formed a honeycomb-like raw image as shown in Fig. 1(right). The raw image consists of an array of sub-images and each sub-image is an image region covered by the corresponding microlens.

B. *Parameter adjustment and components replacement*

In the designed cage-typed light field camera, the parameters such as focal length (*f*), focus distance, optical structure and aberration of the main lens can easily be adjusted. The position of MLA is adjustable as well. The components (MLA, main lens, CCD and relay lens) can be replaced. The effects of parameters adjustment and the components replacement on the raw image are listed below.

(a) Aperture size: The aperture of main lens impacts on the diameter of each sub-image, as shown in Fig. 2. A smaller aperture (larger F-number) would lead to a smaller sub-image and vice versa. Noting that too large aperture leads to the overlap of sub-images [refer to Fig. 2(a)] and it must be avoided.

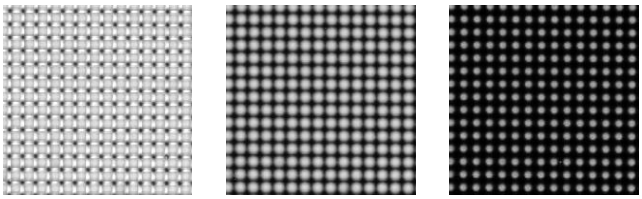

(a) *(b)* *(c)*

Fig. 2. The raw images captured using too large (*a*), appropriate (*b*) and too small aperture (*c*).

(b) Distance (L) from MLA to the virtual image plane: The distance *L* will differ with different positions of MLA in the case that other components are fixed. The different distances will result in different imaging process of the light field camera. Figure 3 shows the raw images captured at different *L*. It can be seen that the same object point projects on different sub-images with the change of magnification, which means a significant change on the optical modulation transfer function and the spatial/angular sampling tradeoff [3]. For the flame, The change of *L* can balance the position resolution of temperature distribution on a longitude-section against the depth resolution between two adjacent sections.

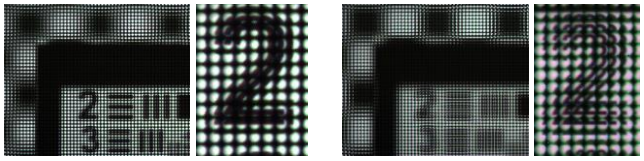

(a) $L < f$ (b) $L > f$

Fig. 3. The raw image with different distances from MLA to the virtual image plane.

(c) Replacement of MLA: The MLA of f/4 is replaced by another MLA of f/15. The diameter of each microlens in MLA of f/15 is greater than that in MLA of f/4. The focal length of the MLA of f/15 is 5 times larger than that in MLA of f/4. The raw image captured by the cage-typed light field camera with the MLA of f/15 is shown in Fig. 4. Comparing with Fig. 1 and Fig. 3, it has been observed that the diameter of each sub-image is increased due to the increased diameter of the microlens, and the checkerboard in the background have lighter blur effects due to the difference of the focal length of MLA. A larger sub-image means dense angular sampling but a sparse spatial sampling, the lighter blur means a deep depth-of-field. For the flame temperature reconstruction, Such a synergistic effect would lead to a disappointed decrease of both position and depth resolution. Thus an MLA with smaller F-number and focal length would be better for the flame detection.

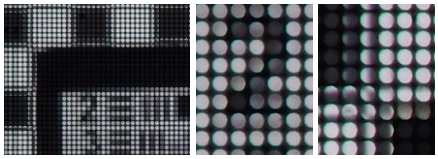

Fig. 4. The raw image with MLA of f/15.

III. CALIBRATION & APPLICATION

The designed cage-type light field camera is applied to study the flame temperature measurement. Due to flame radiation sampling of the light field, the changing of parameters illustrates a great interest in the flame study [6]. In order to apply the cage-typed light field camera to flame temperature measurement, the flame images should be pre-processed before the temperature calculation as follows.

A. *Calibration*

(a) Point spread function (PSF): The raw image of the checkerboard is captured in one depth (distance from the checkerboard to the camera) and then refocused on different positions up to a serious of slopes, which governs the position of a refocus image as a key parameter. Thus, a stack of refocused images is generated with different refocused positions, including the depth of checkerboard. The image refocusing on the checkerboard have the highest sharpness value (calculated using sharpness evaluation function), the slope of this image is then linked to this depth. In this way, the corresponding slope of other depths is determined, as shown in Fig. 5(a). The PSF is then obtained using the solution of the line spread function of refocused image through the edge method.

(b) Intensity calibration: The intensity calibration refers to the relationship between the grey level and the radiation intensity projects on a pixel of CCD sensor as shown in Fig. 5(b). The blackbody furnace is used as a standard radiation source. The radiance intensity is calculated using the Stefan-Boltzmann law. Hence, the relationship is built on the grey level of the image pixel and the temperature value.

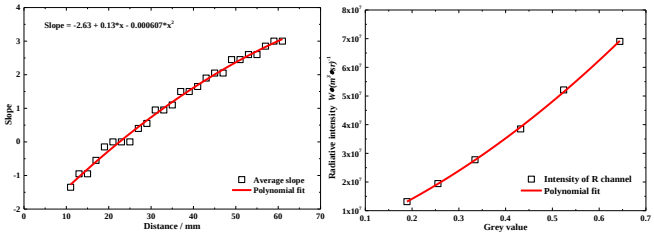

Fig. 5. (a) Slope with refocusing depth and (b) radiance with the grey level of image pixels.

B. *Flame temperature measurement*

Once the raw flame images are captured, the temperature can be calculated as follows:

Step 1 *Image pre-processing:* Firstly, the captured raw images can be processed through demosaic and decoding, which means transfer the 2-D grey value matrix into a 5-D true colour light field database.

Step 2 *Image refocusing:* Refocus the re-processed flame images in different depths.

Step 3 *Deconvolution:* Deconvolve the refocused images to obtain the flame longitude-sections in different depths using the calibrated PSF.

Step 4 *Temperature calculation:* Lastly the flame temperature can be calculated according to the results of intensity calibration using the de-convoluted flame longitude-sections [11].

C. *Priliminary results and discussion*

The cage-typed light field camera is used to capture the candle and ethylene-air diffusion flames simultaneously. Two flame images are located along the cage-typed light field camera. The processed images are shown in Fig. 6.

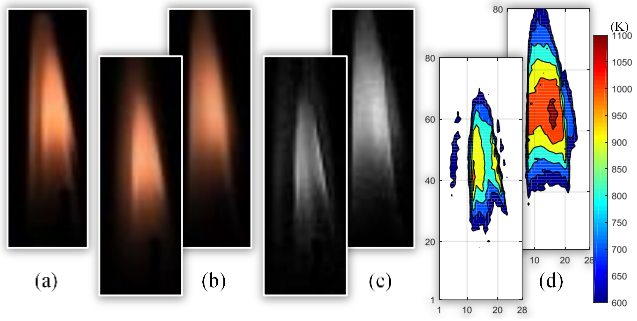

Fig. 6. The depth-of-field-extended image (a), refocused images on the front and back (b), de-convoluted grey level of the two refocused images (c), flame temperature distribution (d).

It can be seen that the two flames show sharp superposition image in the depth-of-field-extended image, while the out-of-focus flame has a blur shade in its corresponding area in the refocused images and the shade can be eliminated in the de-convoluted longitude-sections. The flame temperature is then obtained using the proposed method and shown in Fig. 6(d). The contours show a remarkable shape which is a coincidence to the shape of an in-focus flame. It is worth noting that the out-of-focus flame leaves some measurement errors which can be improved by a more precise PSF calibration. It can also meet a significant improvement while the parameter can be optimised.

IV. Conclusion

A novel cage-typed light field camera was designed and implemented for the study of flame temperature measurement. To evaluate the radiation light field sampling performance, different parameters have been compared based on the raw images. The cage-typed system provided good imaging performance for different parameters, and then be applied to measure the flame temperature. The retrieval results indicate that the proposed system can be useful for the flame temperature measurement. Further work focuses on the analysis of assembling error tolerance and the optimisation of different camera parameters for the flame temperature measurement.

Acknowledgment

This work was supported by the National Natural Science Foundation of China (Nos. 51676044, 51327803) and the Natural Science Foundation of Jiangsu Province for Distinguished Young Scholars (No. BK20150023).

References

[1] A. Gershun, “The light field,” Studies in Applied Mathematics, vol. 18, pp. 51-151, 1939.

[2] R. Ng, M. Levoy, M. Brédif, G. Duval, M. Horowitz, P. Hanrahan, “Light field photography with a hand-held plenoptic camera,” Computer Science Technical Report CSTR, vol. 2.11, pp. 1-11, 2005.

[3] A. Lumsdaine, T. Georgiev, “Focused plenoptic camera and rendering,” Journal of Electronic Imaging, vol. 19, no. 2, pp. 021106, 2010.

[4] X. Guo, H. Lin, Z. Yu, and S. McCloskey, “Barcode Imaging Using a Light Field Camera,” Computer Vision-ECCV 2014 Workshops, Springer International Publishing, pp. 519–532, 2015.

[5] Y. Endo, K. Wakunami, T. Shimobaba, T. Kakue, D. Arai, Y. Ichihashi, K. Yamamoto and T. Ito, “Computer-generated hologram calculation for real scenes using a commercial portable plenoptic camera,” Optics Communications, vol. 356, pp. 468-471, 2015.

[6] J. Sun, C. Xu, B. Zhang, M. Hossain, S. Wang, H. Qi and H. Tan, “Three-dimensional temperature field measurement of flame using a single light field camera,” Optics Express, vol. 24, no. 2, pp. 1118, 2016.

[7] C. Zhang, Z. Ji and Q. Wang, “Decoding and calibration method on focused plenoptic camera,” Computational Visual Media, vol. 2, no. 1, pp. 57-69, 2016.

[8] Lynch, Kyle, Tim Fahringer, and Brian Thurow, “Three-dimensional particle image velocimetry using a plenoptic camera.” 50th AIAA Aerospace Sciences Meeting including the New Horizons Forum and Aerospace Exposition, 2012.

[9] F. Qiang, Z. Zhou, Y. Yuan, B. Xiangli. “Image quality evaluation of light field photography.” IS&T/SPIE Electronic Imaging, International Society for Optics and Photonics, 2011.

[10] C. Niu, H. Qi, X. Huang, L. Ruan and H. Tan, “Efficient and robust method for simultaneous reconstruction of the temperature distribution and radiative properties in absorbing, emitting, and scattering media,” Journal of Quantitative Spectroscopy and Radiative Transfer, vol. 184, pp. 44-57, 2016.

[11] C. Xu, W. Zhao, J. Hu, B. Zhang and S. Wang, “Liquid lens-based optical sectioning tomography for three-dimensional flame temperature measurement,” Fuel, vol. 196, pp. 550-563, 2017.